MISSOURI S&T

Missouri University of Science and Technology

Scholars' Mine

International Specialty Conference on Cold-Formed Steel Structures

(1996) - 13th International Specialty Conference on Cold-Formed Steel Structures

Oct 17th, 12:00 AM

Flexural Strength of Cold-formed Steel Panels Using Structural Grade 80 of A653 Steel

Shaojie Wu

Wei-wen Yu
Missouri University of Science and Technology, wwy4@mst.edu

Roger A. LaBoube
Missouri University of Science and Technology, laboube@mst.edu

Follow this and additional works at: https://scholarsmine.mst.edu/isccss

🎨 Part of the Structural Engineering Commons

Recommended Citation

FLEXURAL STRENGTH OF COLD-FORMED STEEL PANELS USING STRUCTURAL GRADE 80 OF A653 STEEL

Shaojie Wu[1], Wei-Wen Yu[2], and Roger A. LaBoube[3]

ABSTRACT

Cold-formed steel decks made of the Structural Grade 80 of ASTM A653 steel (formerly ASTM A446 Grade E steel) are currently designed according to the AISI specification, using 75% of the specified minimum yield strength of the steel or 60 ksi (413.7 MPa), whichever is less, due to the lack of ductility of the steel. To further evaluate the flexural strength of the cold-formed steel decks using such a steel, a total of seventy-two deck panels with hat-shaped sections were designed and tested under simply supported and two-point loading condition. The test results indicated that for the panel specimens with small w/t ratios (17.93 to 61.07), the tested yield moments were reached and are compared reasonably well with the calculated effective yield moments using actual dimensions, actual yield strength of the steel, and the 1986 AISI Specification. However, for the panel specimens with large w/t ratios (102.86 to 189.95), the tested ultimate moments are lower than the calculated effective yield moments, but much larger than the calculated moments using the specified value of 60 ksi. Fracture in tension was not observed in the tested panels. Panel specimens designed for the first yielding in the tension flange developed higher ratios of tested yield moment to calculated effective yield moment.

1. INTRODUCTION

Cold-formed steel decks have been widely used in buildings as load-carrying structural elements, such as floor and roof decks (Yu 1991, SDI 1992, USD 1994). One of the main structural functions for the steel decks is to carry live and dead loads and transfer the loads to beams or girders. As a result, the decks work as flexural members. The steel decks usually consist of several hat-shaped ribs formed together in their cross section. When such decks, either in single-span or multi-span, is subject to uniform or concentrated loads, the overall stability of the decks, such as lateral torsional buckling, often does not control the moment capacity of the members.

In the United States, it is a common practice that steel decks are made of the Structural Grade 80 of ASTM A653 steel (formerly ASTM A446 Grade E steel). The unique property of the Structural Grade 80 steel, as compared to the conventional steels used for cold-formed

1. Post-Doctoral Fellow, Department of Civil Engineering, University of Missouri-Rolla, Rolla, MO 65401.

2. Curators' Professor Emeritus of Civil Engineering, University of Missouri-Rolla, Rolla, MO 65401.

3. Associate Professor of Civil Engineering, University of Missouri-Rolla, Rolla, MO 65401.

members, is that it has a high specified yield strength (F_y=80 ksi (551.6 MPa) and a low tensile-to-yield strength ratio (F_u/F_y=1.03). The ductility of the steel is unspecified (ASTM A446) and was reported to be smaller than the ductility requirements for the conventional steels (Dhalla and Winter 1971).

Due to the lack of ductility and low tensile-to-yield strength ratio of the Structural Grade 80 steel and considering the required ductility for adequate structural performance, Section A3.3.2 of the specifications for the design of cold-formed steel structural members (AISI 1986, AISI 1991) permits the use of the steel for particular configurations provided that (1) the yield strength, F_y, used for design of elements, members, and structural assemblies, is taken as 75% of the specified minimum yield point or 60 ksi (413.7 MPa), whichever is less, and (2) the tensile strength, F_u, used for design of connections and joints, is taken as 75% of the specified minimum tensile strength or 62 ksi (427.5 MPa), whichever is less.

In the past, studies on the strength and performance of structural components made of the Structural Grade 80 steel were limited (Wu, Yu, and LaBoube 1995). The reduction of the specified material properties by 25% for design purposes is based on the fact that the structural performance of cold-formed members and connections made of such a steel has not been fully investigated and understood. Therefore, since 1995, a research project on the strength of flexural members using Structural Grade 80 of A653 steel has been carried out at the University of Missouri-Rolla to further study the strength and performance of flexural members and connections made of such a steel. This paper summarizes the results of the panel tests under two-point loading and simply supported condition. Panel tests under one-point loading condition, web crippling tests, and connection tests are planned for further study.

2. MATERIAL TESTS

To determine the ductility and material properties of the Structural Grade 80 steel and to use them to evaluate the results of panel tests, a total of seventy-six tensile coupon tests were conducted (Wu, Yu, and LaBoube 1995). The tensile coupons were made of 22, 24, 26, and 28 gage steel sheets and cut both parallel and perpendicular to the rolling direction of the sheets. The results of the tensile coupon tests are shown in Table 1. It is noted in the table that with decreases in thickness of the steel sheets, the yield and tensile strengths increase, but the ductility tends to decrease. In the direction perpendicular to the rolling direction, the 0.2% offset yield strength and tensile strength of the sheets are much higher than those in the rolling direction, while the ductility is much lower than those in the rolling direction.

3. DESIGN OF PANEL SPECIMENS

Twenty-four hat-shaped sections were designed based on the actual yield strength of the Structural Grade 80 steel and the AISI Specification (AISI 1986). The design parameters include: thickness, flange flat-width-to-thickness ratio (w/t), web flat-width-to-thickness ratio (h/t), and extreme fiber tension-to-compression stress ratio (f_t/f_c) at first yielding in a section. Three types of steel sheets were used, namely 22, 26, and 28 gage sheets. The designed w/t ratios ranged from 17.24 to 189.66 and the h/t ratios ranged from 17.24 to 103.45, which were selected based on current cold-formed steel deck products (USD 1994, SDI 1992). Three f_t/f_c ratios, namely 0.8,

1.0, and 1.2, were used for (1) first yielding in compression flange only, (2) in both compression and tension flanges simultaneously, and (3) in tension flange only, respectively. The designed inside bend radius, R, was taken as 1/16 inches (1.59 mm) for all four steel sheets, which results in a R/t ratio ranging from 2.16 to 4.17. The designed angle between the plane of the web and the plane of the bearing surface, θ, was taken as 60 degree. Table 2 illustrates the variation of the w/t and h/t ratios used for the design of the twenty-four sections, and Figure 1 shows the shape of the sections. In the table, each combination of w/t and h/t ratios corresponds to three f_t/f_c ratios (0.8, 1.0, and 1.2).

For each of the twenty-four sections, three panel specimens were fabricated. After the members were manufactured from long sheets, three panel specimens and a segment were cut from the members representing each section. The dimensions of each segment were carefully measured using a calliper with an accuracy of 0.001 inches (0.025 mm). The angle between planes of the web and adjacent flanges was measured twice using an angular ruler, one with respect to the compression flange and the other with respect to tension flange. The measured dimensions of all elements and the angles of all webs are shown in Tables 3, 4, and 5, and the shape of the sections is shown in Figure 2. In these tables, each specimen is designated as: t**w**h**-*(x), where "t**" represents gage number (thickness), such as t22 (22 gage); "w**" indicates the flat width of the compression flange, such as w1.5 (w=1.5 inches (38.1 mm)); "h**" represents the flat width of the web, such as h1 (h=1.0 inch (25.4 mm)); "-*" indicates the location of the first yielding, such as -c (occurring in compression flange only); -ct (in compression and tension flanges simultaneously); and -t (in tension flange only). "(x)" represents test number such as 1, 2, and 3. The actual inside bend radius, R, was 1/32 inches (0.79 mm) in all specimens. The actual w/t ratios ranged from 17.18 to 189.95 and the actual h/t ratios ranged from 16.35 to 104.89.

With all the measured dimensions, effective yield moments were calculated for all sections using the computer program CFS (Glauz 1990) and the actual yield strength of the steel. The average value of the two measured angles between the web and the two flanges was used in the calculation. The shear strength of webs, shear-moment interaction, web crippling strength of webs, web crippling-moment interaction, and shear lag were checked using the AISI Specification (AISI 1986) to determine the total length of each panel specimen so that no other failure modes will be possible during a test except the flexural failure mode.

4. TEST SETUP, INSTRUMENTATION, AND TEST PROCEDURE

Each panel specimen was placed on two simple supports (one was a roller condition and the other was a pin condition) which were fastened on a wide flange support beam 84 inches (2134 mm) long. The support beam was firmly connected to the platen of the MTS 880 loading frame located at the Engineering Research Laboratory at the University of Missouri-Rolla. A cross beam was used to establish a two-point loading condition, with one pin and one roller at each end of the beam. Load was applied to the center of the cross beam. For all the tests, the distance between a support of a panel and the load transferred from one end of the cross beam ranged from L/6 to L/3.11 (L is the span length of the panel between two supports). Bracing was attached to the tension flanges of panel specimens using C-clamps at several locations along the entire length of all specimen to prevent the section from changing its shape. The test setup is

shown in Figure 3. Displacement control was used to load a specimen throughout the test with a displacement rate of 0.000125 inches (0.0032 mm) per second. The displacement control was carried out automatically through the MTS 880 control system.

Two LVDTs were used to record the displacements at the center of the panel specimen, with each LVDT on each side of the specimen. Two additional LVDTs were located at the two loading locations. Twelve to eighteen strain gages were used throughout the constant moment region to record top and bottom extreme fiber strains and to detect initiation of local buckles. All of the LVDT and strain gage data were simultaneously recorded through a CMAC data acquisition system with a sampling rate of three samples per second.

Before a panel specimen was loaded, the initial readings of the LVDTs and strain gages were recorded. The cross beam was placed and the readings of the LVDTs and strain gages were recorded again. The displacement control mode of the MTS system was then started immediately after continuous data recording was initiated. After the specimen had failed, the displacement control mode was terminated while the data recording continues until the cross beam was automatically and gradually released from the upper platen of the MTS 880 system.

5. TEST RESULTS

Seventy-two panel specimens were tested, which involved twenty-four different sections as shown in Tables 2, 3, and 4. For each section, three panel specimens were tested. The following is a brief summary of the test results and the behavior of the panel specimens.

(1) Panel specimens t28w1.5h1-c(1,2,3), t28w1.5h1-ct(1,2,3), and t28w1.5h1-t(1,2,3): Flange local buckling occurred at about a quarter of the yield load. More than half of the panels yielded in the section. All the panels failed suddenly due to the formation of a local failure mechanism in the constant moment region shortly after ultimate load was reached. Local buckles of the flanges and webs largely developed at ultimate load in all the panels. The maximum ratio of central deflection to span at ultimate load was 1/22.

(2) Panel specimens t26w0.5h0.5-c(1,2,3), t26w0.5h0.5-ct(1,2,3), and t26w0.5h0.5-t(1,2,3): Flange local buckling occurred shortly prior to yielding. All of the panels yielded in the section. A plateau in the load vs. central deflection curve was developed for all the panels prior to a sudden failure due to the formation of a local failure mechanism in the constant moment region. Local buckles of the flanges and webs largely developed prior to failure. The maximum ratio of central deflection to span prior to failure was about 1/12.

(3) Panel specimens t26w1h0.75-c(1,2,3), t26w1h0.75-ct(1,2,3), and t26w1h0.75-t(1,2,3): Flange local buckling occurred at about half of the yield load. The majority of the panels yielded in the section. A plateau in the load vs. central deflection curve was developed especially for the panels designed for first yielding in tension flange. All the panels failed suddenly due to the formation of a local failure mechanism in the constant moment region. Local buckles of the flanges and webs largely developed prior to failure. The maximum ratio of central deflection to span prior to failure was about 1/15.

(4) Panel specimens t26w2h1.5-c(1,2,3), t26w2h1.5-ct(1,2,3), and t26w2h1.5-t(1,2,3): Flange local buckling occurred at about one-fifth of the yield load. Less than half of the panels yielded in the section. All the panels failed suddenly due to the formation of a local failure mechanism in the constant moment region. Local buckles of the flanges and webs largely developed prior to failure. The maximum ratio of central deflection to span prior to failure was 1/31.

(5) Panel specimens t22w0.5h0.5-c(1,2,3), t22w0.5h0.5-ct(1,2,3), and t22w0.5h0.5-t(1,2,3): All the panels yielded in the section and continued to carry additional load beyond first yielding until an ultimate load was reached. Shortly prior to reaching an ultimate load, sections within one of the braced segments tended to open up (change shape). After the ultimate load was reached, the decrease in applied load was small with further increase in displacement. Tests were terminated because of excessively large displacement. A large plateau in the load vs. central deflection curve was developed for the panels having the sections of t22w0.5h0.5-ct and t22w0.5h0.5-t. No local buckling occurred at yielding. Sudden formation of a local failure mechanism did not occur before test was terminated. The panels showed sufficient ductility.

(6) Panel specimens t22w1h0.75-c(1,2,3), t22w1h0.75-ct(1,2,3), and t22w1h0.75-t(1,2,3): Flanges buckled locally shortly before yielding in all the panels. The majority of the panels yielded in the section and continued to carry additional load beyond first yielding. A plateau in the load vs. central deflection curve was developed in all the panels before a local failure mechanism formed gradually within the constant moment region. Local buckles developed slightly prior to failure only in the flanges. The maximum ratio of central deflection to span was 1/16 prior to failure.

(7) Panel specimens t22w3h2-c(1,2,3), t22w3h2-ct(1,2,3), and t22w3h2-t(1,2,3): Flanges buckled locally at about a quarter of the yield load in all the panels. The majority of the panels yielded in the section, especially for the sections of t22w3h2-ct and t22w3h2-t. A plateau in the load vs. central deflection curve was developed in the panels having the sections of t22w3h2-ct and t22w3h2-t before a local failure mechanism suddenly formed in the constant moment region. Local buckles largely developed in the flanges and webs prior to failure. The maximum ratio of central deflection to span was about 1/37 prior to failure.

(8) Panel specimens t22w5.5h3-c(1,2,3), t22w5.5h3-ct(1,2,3), and t22w5.5h3-t(1,2,3): Flanges buckled shortly after load was applied. Only two panels indicated yielding in the section, but the maximum strains were well above 4000 micro strain prior to failure for the rest of the other panels. This strain level corresponded to about 95 ksi (655.0 MPa) stress in the section based on the material test. All of the panels failed suddenly due to the formation of a local failure mechanism in the constant moment region. The maximum ratio of central deflection to span was about 1/47 prior to failure.

Comparing all the tested panel specimens, most of the panel specimens with the w/t ratios of 103.52 or less experienced yielding in the section and continued to yield after first yielding, while with further increases in the w/t ratios (larger than 103.52), the number of the panel specimens undergoing yielding in the section decreased. Even though some panels did not indicate yielding in the section prior to failure, the ultimate strains in almost all the panels exceeded 4000 micro strain. This strain level corresponded to at least 95 ksi stress (655.0 MPa)

in the three types of steel sheets based on the material tests. With increases in the w/t ratios, the magnitude of the ultimate strains decreased. The maximum central deflection prior to the failure of panel specimens is always the largest for the sections designed with first yielding in tension flange and the smallest for the sections designed with first yielding in compression flange. All of the recorded ultimate strains were less than 1.4% in./in. and no tensile fracture was observed in the tested panels.

6. EVALUATION OF TEST RESULTS

The flexural strengths of the seventy-two tested panel specimens were evaluated and compared to those predicted by using the AISI Specification (AISI 1986) and the measured dimensions. The effective moments were calculated using the actual yield strength, 75% of the actual yield strength, and the specified 60 ksi (413.7 MPa) for the Structural Grade 80 steel. The modulus of elasticity was taken as 29500 ksi (203 GPa) for all the calculations. The results of evaluation are discussed as follows.

The effective moment calculated by using the specified 60 ksi (equal to 75% of the specified minimum yield strength (80 ksi (551.6 MPa)) for the Structural Grade 80 steel) is compared to the average tested ultimate moment of three panel specimens for each section (listed in Tables 3, 4, and 5) as shown in Figure 4 and Table 6. Figure 4 shows that for all the panel sections considered in this study, the ratio of the average tested ultimate moment to the calculated effective moment using the 60 ksi is larger than 1.2. This indicates that the predicted flexural strength of cold-formed steel decks made of the Structural Grade 80 steel by using the specified 60 ksi stress is conservative. The moment ratios tend to decrease with increases in the w/t ratios.

Figure 4 and Table 6 also show the ratios of the average tested ultimate moment to the calculated effective moment by using 75% of the actual yield strength against the w/t ratios. It is clear in the figure that the moment ratios are all larger than 1.0 for the w/t ratios considered in the tests. As a result, the predicted flexural strength of the panels using 75% of the actual yield strength is also conservative, especially for the low w/t ratios.

The tested ultimate moments are also compared with the effective yield moments calculated by using the actual yield strength of the steel as shown in Table 7 and Figure 5 for all the tested panels. The figure indicates that the ratio of the tested ultimate moment to the calculated effective yield moment using the actual yield strength decreases from 1.25 to about 0.80 with increases in the w/t ratios. The moment ratios are usually larger than 1.0 for the w/t ratios of 61.07 or less, and less than 1.0 for the w/t ratios of 102.86 or larger, with a tendency to converge to 0.85 at larger w/t ratios (120 to 190). It is also noted from Figure 5 that the highest moment ratios tend to be achieved for the sections designed with first yielding in tension flange as compared to the sections designed with first yielding in compression flange and in both compression and tension flanges.

A comparison between the tested yield moments and the calculated effective yield moments using the actual yield strength of the steel is shown in Table 8 and Fig. 6. Similar to what is observed in Fig. 5, the ratio of the tested yield moment to the calculated effective yield moment by using the actual yield strength of the steel decreases with increases in the w/t ratios,

with a tendency of converging to 0.80 at the larger w/t ratios (120 to 190). The lower moment ratios correspond to the panels with the larger w/t ratios, in which the chance of yielding in a section is small. The tested yield moments are predicted reasonably well by the calculated effective yield moments for the w/t ratios of 61.07 or less. Figure 6 also indicates that larger moment ratios tend to be achieved with the panel sections designed for the first yielding occurred in tension flanges.

Due to the fact that the ultimate strains in panels made of high strength steel and having larger w/t ratios are often lower than the yield strain, the equation, developed by Pan (1987) to account for a yield strength reduction factor in predicting the effective moment, was used to predict the effective moments of the panel sections designed for the first yielding in compression flange and in both compression and tension flanges. Figure 7 shows the ratios of the tested yield moment to the effective moment calculated using the yield strength reduction factor against the w/t ratios. It is noted from the figure that a slight improvement in predicting the yield moment is achieved with the use of the reduction factor for the sections having the w/t ratios of 102.86 or larger, however, the prediction using the reduction factor is conservative for the sections with the w/t ratios of 61.07 or less, as compared to the moment ratios shown in Fig. 6.

7. SUMMARY

A total of seventy-two cold-formed steel panels, involving twenty-four different hat-shaped sections and made of the Structural Grade 80 of ASTM A653 steel sheets, were tested under simply supported and two-point loading conditions. The preliminary research findings and the evaluation of the results are summarized as follows:

(1) Yield strains were recorded in the panels with the w/t ratios ranging from 17.93 to 189.95, however, the number of the panels that experienced yielding decreases with the w/t ratio of 118.64 or larger, while yielding occurred in the majority of the panels with the w/t ratio of 103.52 or less. Ultimate strains prior to failure of the panels were much larger than the yield strains in the majority of the panels with the w/t ratio of 103.52 or less. The specimens without flange local buckling showed sufficient ductility. Fracture in tension was not observed in the tested panel specimens. For details, refer to Wu, Yu, and LaBoube (1996).

(2) For the panels with the w/t ratio of 61.07 or less, the tested yield moments compared reasonably well with the calculated effective yield moments by using the actual panel dimensions, actual yield strength of the steel, and the 1986 AISI Specification. However, for the panels with the w/t ratio of 102.86 or larger, the tested ultimate moments were lower than the calculated effective yield moments using the actual yield strength, but larger than the calculated moments using the 60 ksi stress or 75% of the actual yield strength. It was found to be conservative to predict the effective moment using the specified 60 ksi stress for the cold-formed steel panels made of the Structural Grade 80 of ASTM A653 steel. This is justified by the fact that the ultimate strains in almost all the panels were larger than 4000 micro strain which corresponded to at least 95 ksi (655.0 MPa) in the three types of steel sheets.

(3) The tested ultimate moments are larger than the calculated effective yield moments for the majority of the panels having the w/t ratio of 61.07 or less, indicating a potential inelastic reserve

capacity as justified by the recorded higher ultimate strains.

(4) Panel specimens which were designed for the first yielding in the tension flange developed a higher ratio of the tested ultimate moment, or yield moment, to the calculated effective yield moment.

(5) The equation, developed by Pan (1987) to account for a yield strength reduction factor in predicting the effective moment of flexural members made of high strength steel, slightly improves the prediction of effective moment for the panels with the w/t ratio of 102.86 or larger, but was found to be conservative for the panels with the w/t ratio of 61.07 or less. For details, refer to Wu, Yu, and LaBoube (1996).

(6) The low ductility of the Structural Grade 80 of ASTM A653 steel does not appear to have adversely affected the flexural strength of the tested panels. This may be due to the fact that recorded ultimate strains in the panels were much less than the percent elongation in a 2-inch (50.8 mm) gage length of the steel.

ACKNOWLEDGEMENT

APPENDIX I. REFERENCES

American Iron and Steel Institute, (1991). "Load and Resistance Factor Design Specification for Cold-Formed Steel Structural Members." March 16, 1991 Edition.

American Iron and Steel Institute. (1986). "Specification for the Design of Cold-Formed Steel Structural Members." August 19, 1986 Edition with the December 11, 1989 Addendum.

ASTM A446. "Standard Specification for Steel Sheet, Zinc-Coated (Galvanized) by the Hot-Dip Process, Physical (Structural Quality." Annual Book of ASTM Standards.

Dhalla, A.K., and Winter, G. (1971). "Influence of Ductility on the Structural Behavior of Cold-formed Steel Members." Report No. 336, Cornell University, June.

Glauz, R.S. (1990). "Cold-Formed Steel Design Program, User's Manual."

Pan, L.C. (1987). "Effective Design Widths of High Strength Cold-Formed Steel Members."

Ph.D. Dissertation, Department of Civil Engineering, University of Missouri-Rolla, Rolla, MO.

Steel Deck Institute (SDI). (1992). "Steel Deck Institute Design Manual for Composite Decks, Form Decks, Roof Decks, and Cellular Metal Floor Deck with Electrical Distribution." Steel Deck Institute, Publication No. 28.

United Steel Deck (USD). (1994). "Steel Decks for Floors and Roofs, Design Manual and Catalog of Products." Nicholas J. Bouras, Inc.

Wu, S., Yu, W.W., and LaBoube, R.A. (1995). "Strength of Flexural Members Using Structural Grade 80 of A653 and Grade E of A611 Steels." First Progress Report, Civil Engineering Study 95-5, Department of Civil Engineering, University of Missouri-Rolla, Rolla, MO.

Wu, S., Yu, W.W., and LaBoube, R.A. (1996). "Strength of Flexural Members Using Structural Grade 80 of A653 and Grade E of A611 Steels." Second Progress Report (To be published), Department of Civil Engineering, University of Missouri-Rolla, Rolla, MO.

Yu, W.W. (1991). "Cold-Formed Steel Design." Second Edition, John Wiley & Sons, Inc.

APPENDIX II. NOTATIONS

The following symbols are used in this paper:

F_y = specified yield strength of cold-formed sheet steel.
F_u = specified tensile strength of cold-formed sheet steel.
f_t/f_c = ratio of the tensile to the compressive stress.
h = flat width of web.
L = span length, measured between centers of two supports of the panel.
R = inside bend radius.
t = thickness of panel sheet.
w = flat width of compression flange.
θ = angle between planes of the web and bearing surface.

Table 1 Material Properties of 22, 24, 26, and 28 Gage Steel Sheets

Direction	Gage	Thickness (in.)	0.2% Offset Yield Strength F_y (ksi)	Tensile Strength F_u (ksi)	Tensile-to-Yield Ratio F_u/F_y	Local Elongation in 1/2-in Gage Length (%)	Uniform Elongation Outside Fracture (%)	Elongation in 2-in Gage Length (%)
Parallel to Rolling Direction	22	0.029	103.9	107.7	1.04	11.98	1.29	3.67
	24	0.024	110.1	116.4	1.06	9.33	1.23	2.69
	26	0.017	112.5	115.9	1.03	9.13	0.77	2.40
	28	0.015	111.0	116.1	1.05	7.89	1.04	2.77
Perpendicular to Rolling Direction	22	0.029	119.6	121.2	1.02	7.29	0.41	1.99
	24	0.024	126.0	128.5	1.02	6.40	0.35	1.78
	26	0.017	129.7	132.6	1.02	3.78	0.43	1.32
	28	0.015	127.3	130.1	1.02	3.78	0.43	1.38

Note: All the steel sheets were made of the Structural Grade 80 of ASTM A653 Steel. 1 inch = 25.4 mm. 1 ksi = 6.895 MPa.

Table 2 w/t and h/t Ratios Used for the *Design* of Panel Specimens

t (gage#) (inches)	w (inches)					
	0.5	1.0	1.5	2	3	5.5
0.015 (28)	--	--	100.00	--	--	--
0.017 (26)	29.41	58.82	--	117.65	--	--
0.029 (22)	17.44	34.48	--	--	103.45	189.66
t (gage #) (inches)	h (inches)					
	0.5	0.75	1.0	1.5	2.0	3.0
0.015 (28)	--	--	66.67	--	--	--
0.017 (26)	29.41	44.12	--	88.24	--	--
0.029 (22)	17.24	25.86	--	--	68.97	103.45
f_t/f_c	0.8,1.0,1.2	0.8,1.0,1.2	0.8,1.0,1.2	0.8,1.0,1.2	0.8,1.0,1.2	0.8,1.0,1.2

Note: see Figure 1 for the measurement of w and h. 1 inch = 25.4 mm.

Figure 1 Cross Section Used for the *Design* of Panel Specimens

Table 3 Measured Dimensions of Panel Specimens Made of 28 Gage Sheet Steel

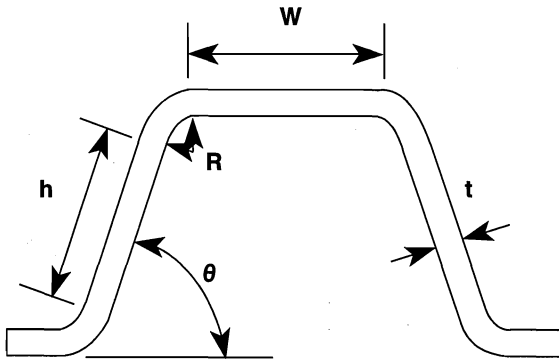| Section Type of Specimen (#)	$L_{1,2}$ (in.)	$L_{2,3}$ (in.) ($\theta_{2,3}$ in degree)	$L_{3,4}$ (in.)	$L_{4,5}$ (in.) ($\theta_{4,5}$ in degree)	$L_{5,6}$ (in.)	$L_{6,7}$ (in.) ($\theta_{6,7}$ in degree)	$L_{7,8}$ (in.)	$L_{8,9}$ (in.) ($\theta_{8,9}$ in degree)	$L_{9,10}$ (in.)	$L_{10,11}$ (in.) ($\theta_{10,11}$ in degree)	$L_{11,12}$ (in.)	$L_{12,13}$ (in.) ($\theta_{12,13}$ in degree)	$L_{13,14}$ (in.)
t28w1.5h1-c (1)	0.469	1.094 (60,60)	1.594	1.085 (63,58)	0.865	1.091 (58,62)	1.607	1.053 (59,61)	0.465	--	--	--	--
t28w1.5h1-ct (2)	0.271	1.085 (62,62)	1.585	1.083 (63.5,59)	0.472	1.105 (59,62)	1.630	1.036 (61,61)	0.268	--	--	--	--
t28w1.5h1-t (3)	0.222	1.062 (64,59)	1.578	1.085 (62,60)	0.348	1.098 (62.5,63.5)	1.619	1.034 (64.5,61)	0.218	--	--	--	--

Note: see Figure 2 for measurement of dimensions. 1 inch = 25.4 mm.
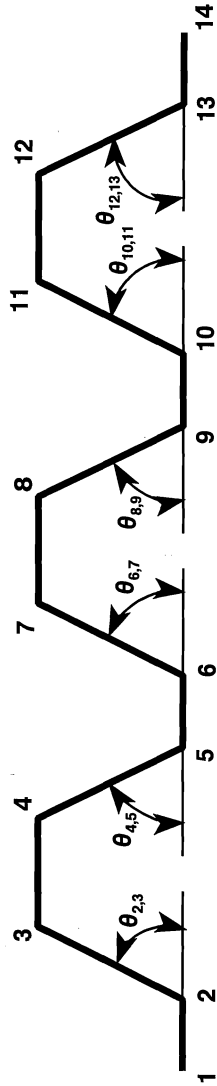
Figure 2 Cross Section of Panel Specimen

Table 4 Measured Dimensions of Panel Specimens Made of 26 Gage Sheet Steel (see Figure 2 for Dimensions)

Type of Specimen (#)	$L_{1,2}$ (in.)	$L_{2,3}$ (in.) ($\theta_{2,3}$ in degree)	$L_{3,4}$ (in.)	$L_{4,5}$ (in.) ($\theta_{4,5}$ in degree)	$L_{5,6}$ (in.)	$L_{6,7}$ (in.) ($\theta_{6,7}$ in degree)	$L_{7,8}$ (in.)	$L_{8,9}$ (in.) ($\theta_{8,9}$ in degree)	$L_{9,10}$ (in.)	$L_{10,11}$ (in.) ($\theta_{10,11}$ in degree)	$L_{11,12}$ (in.)	$L_{12,13}$ (in.) ($\theta_{12,13}$ in degree)	$L_{13,14}$ (in.)
t26w05h0.5-c (4)	0.365	0.589 (61, 60)	0.584	0.566 (60.5,60)	0.748	0.585 (60,60.5)	0.574	0.581 (60,61)	0.748	0.591 (60,61)	0.614	0.562 (62,61.5)	0.375
t26w0.5h0.5-ct (5)	0.242	0.596 (61,59.5)	0.588	0.560 (61.5,60)	0.499	0.585 (60.5,61.5)	0.570	0.575 (61,60.5)	0.494	0.593 (58,61)	0.598	0.572 (61,62)	0.254
t26w0.5h0.5-t (6)	0.218	0.564 (61.5,60.5)	0.585	0.549 (62,63)	0.391	0.597 (60.5,61.5)	0.574	0.575 (60,62)	0.377	0.591 (60,61.5)	0.630	0.510 (70,64)	0.220
t26w1h0.75-c (7)	0.434	0.843 (62,62)	1.071	0.828 (63.5,62)	0.854	0.844 (61,61)	1.121	0.813 (60.5,63)	0.452	--	--	--	--
t26w1h0.75-ct (8)	0.283	0.821 (58.5,57.5)	1.072	0.834 (61,61.5)	0.577	0.834 (58,58.5)	1.090	0.841 (56.5,61)	0.273	--	--	--	--
t26w1h0.75-t (9)	0.209	0.804 (61,64)	1.077	0.824 (62,62)	0.344	0.830 (60,60.5)	1.063	0.813 (60,63)	0.212	--	--	--	--
t26w2h1.5-c (10)	0.483	1.594 (63.5,59)	2.072	1.578 (60,59)	0.889	1.596 (62,64)	2.136	1.521 (63,59.5)	0.489	--	--	--	--
t26w2h1.5-ct (11)	0.289	1.590 (62.5,57)	2.067	1.580 (59.5,58)	0.529	1.610 (62,63)	2.079	1.568 (62.5,58.5)	0.298	--	--	--	--
t26w2h1.5-t (12)	0.214	1.562 (61.5,62.5)	2.073	1.578 (64,62.5)	0.340	1.602 (59,60.5)	2.084	1.538 (60.5,65)	0.221	--	--	--	--

Table 5 Measured Dimensions of Panel Specimens Made of 22 Gage Sheet Steel (see Figure 2 for Dimensions)

Section Type of Specimen (#)	$L_{1,2}$ (in.)	$L_{2,3}$ (in.) ($\theta_{2,3}$ in degree)	$L_{3,4}$ (in.)	$L_{4,5}$ (in.) ($\theta_{4,5}$ in degree)	$L_{5,6}$ (in.)	$L_{6,7}$ (in.) ($\theta_{6,7}$ in degree)	$L_{7,8}$ (in.)	$L_{8,9}$ (in.) ($\theta_{8,9}$ in degree)	$L_{9,10}$ (in.)	$L_{10,11}$ (in.) ($\theta_{10,11}$ in degree)	$L_{11,12}$ (in.)	$L_{12,13}$ (in.) ($\theta_{12,13}$ in degree)	$L_{13,14}$ (in.)
t22w05h0.5-c (13)	0.472	0.598 (60,62.5)	0.596	0.554 (62,63.5)	0.979	0.602 (60.5,61)	0.568	0.587 (59,60)	0.946	0.599 (62,60.5)	0.628	0.564 (63,63)	0.469
t22w0.5h0.5-ct (14)	0.319	0.601 (59,60)	0.587	0.563 (61,61)	0.664	0.602 (58,59)	0.583	0.577 (57.5,58.5)	0.644	0.607 (61,59)	0.634	0.545 (61,61)	0.316
t22w0.5h0.5-t (15)	0.233	0.581 (61,61.5)	0.583	0.565 (62,61)	0.457	0.600 (60.5,60.5)	0.571	0.594 (60,61.5)	0.445	0.607 (62,60)	0.619	0.559 (61,62.5)	0.233
t22w1h0.75-c (16)	0.612	0.842 (59,60)	1.086	0.841 (60.5,59)	1.205	0.864 (58.5,58)	1.084	0.833 (58,60.5)	0.625	-	-	-	-
t22w1h0.75-ct (17)	0.414	0.845 (59,61)	1.084	0.838 (61.5,61.5)	0.867	0.854 (59.5,58.5)	1.111	0.811 (65,61.5)	0.411	-	-	-	-
t22w1h0.75-t (18)	0.270	0.841 (59.5,60)	1.084	0.847 (61,62)	0.534	0.846 (60,59)	1.088	0.843 (58,62.5)	0.286	-	-	-	-
t22w3h2-c (19)	0.860	2.095 (59.5,59.5)	3.066	2.085 (60,61)	0.864	-	-	-	-	-	-	-	-
t22w3h2-ct (20)	0.474	2.104 (60.5,62)	3.059	2.081 (59.5,64.5)	0.496	-	-	-	-	-	-	-	-
t22w3h2-t (21)	0.292	2.106 (61,64)	3.068	2.075 (62,60)	0.313	-	-	-	-	-	-	-	-
t22w5.5h3-c (22)	0.738	3.097 (62.5,60.5)	5.552	3.103 (61,62)	0.739	-	-	-	-	-	-	-	-
t22w5.5h3-ct (23)	0.445	3.112 (60.5,60.5)	5.573	3.078 (60.5,61.5)	0.460	-	-	-	-	-	-	-	-
t22w5.5h3-t (24)	0.296	3.112 (61,60)	5.579	3.032 (59.5,62)	0.313	-	-	-	-	-	-	-	-

Table 6 Calculated Moments Using Specified 60 ksi Stress, 75% Actual Yield Strength and 100% of Actual Yield Strength

Sections	Thickness (in.)	Average w/t	$M_{e,60ksi}$ (kips-in)	$M_{e,75\%Fy}$ (kips-in)	$M_{y,100\%Fy}$ (kips-in)	f_c/f_t (100%F$_y$)
t28w1.5h1-c	0.015	103.13	1.68	2.16	2.78	0.81
t28w1.5h1-ct	0.015	103.52	1.38	1.91	2.44	1.05
t28w1.5h1-t	0.015	102.86	1.26	1.75	2.22	1.10
t26w0.5h0.5-c	0.017	31.43	1.08	1.43	1.80	0.84
t26w0.5h0.5-ct	0.017	31.33	0.90	1.27	1.69	1.00
t26w0.5h0.5-t	0.017	31.65	0.84	1.10	1.46	1.08
t26w1h0.75-c	0.017	61.07	1.38	1.77	2.25	0.83
t26w1h0.75-ct	0.017	60.38	1.14	1.60	2.03	1.00
t26w1h0.75-t	0.017	59.56	0.96	1.35	1.80	1.13
t26w2h1.5-c	0.017	120.41	3.42	4.47	5.40	0.84
t26w2h1.5-ct	0.017	118.64	2.94	4.05	5.18	0.98
t26w2h1.5-t	0.017	118.86	2.64	3.63	4.84	1.09
t22w0.5h0.5-c	0.029	18.13	1.86	2.42	3.22	0.84
t22w0.5h0.5-ct	0.029	18.35	1.68	2.18	2.91	1.00
t22w0.5h0.5-t	0.029	17.93	1.50	1.95	2.60	1.12
t22w1h0.75-c	0.029	35.06	3.00	3.66	4.57	0.80
t22w1h0.75-ct	0.029	35.40	2.64	3.43	4.47	1.00
t22w1h0.75-t	0.029	35.04	2.10	2.65	3.53	1.24
t22w3h2-c	0.029	103.33	6.00	7.40	9.35	0.80
t22w3h2-ct	0.029	103.00	5.28	6.70	8.73	1.00
t22w3h2-t	0.029	103.31	4.32	5.53	7.17	1.19
t22w5.5h3-c	0.029	188.98	10.68	13.17	14.86	0.79
t22w5.5h3-ct	0.029	189.74	9.18	11.69	15.07	0.99
t22w5.5h3-t	0.029	189.95	7.98	10.13	13.30	1.13

Note: 1 inch = 25.4 mm. 1 kip = 4.448 kN. $M_{e,60ksi}$ = Effective moment calculated by using 60 ksi stress. $M_{e,75\%Fy}$ = Moment calculated by using 75% of the actual yield strength. $M_{y,100\%Fy}$ = Yield moment calculated by using 100% of the actual yield strength. f_c/f_t = calculated tension to compression stress ratio. All the moments are calculated based on the AISI Specification (AISI 1986).

Table 7 Tested Ultimate Moments and Ratios of Tested Ultimate Moment to Calculated Yield Moment

Specimens	Thickness (in.)	Average w/t	$M_{u,test}$ (kips-in) (test 1)	$M_{u,test}$ (kips-in) (test 2)	$M_{u,test}$ (kips-in) (test 3)	$M_{u,test}/M_{y,100\%Fy}$ (test 1)	$M_{u,test}/M_{y,100\%Fy}$ (test 2)	$M_{u,test}/M_{y,100\%Fy}$ (test 3)
t28w1.5h1-c(1,2,3)	0.015	103.13	2.41	2.40	2.37	0.87	0.86	0.85
t28w1.5h1-ct(1,2,3)	0.015	103.52	2.32	2.35	2.32	0.95	0.96	0.95
t28w1.5h1-t(1,2,3)	0.015	102.86	2.20	2.19	2.13	0.99	0.99	0.96
t26w0.5h0.5-c(1,2,3)	0.017	31.43	1.79	1.83	1.85	0.99	1.02	1.03
t26w0.5h0.5-ct(1,2,3)	0.017	31.33	1.80	1.97	1.78	1.07	1.17	1.05
t26w0.5h0.5-t(1,2,3)	0.017	31.65	1.64	1.81	1.66	1.12	1.24	1.14
t26w1h0.75-c(1,2,3)	0.017	61.07	2.32	2.33	2.35	1.03	1.04	1.04
t26w1h0.75-ct(1,2,3)	0.017	60.38	2.33	2.23	2.25	1.15	1.10	1.11
t26w1h0.75-t(1,2,3)	0.017	59.56	2.13	2.16	2.12	1.18	1.20	1.18
t26w2h1.5-c(1,2,3)	0.017	120.41	4.50	4.54	4.59	0.83	0.84	0.85
t26w2h1.5-ct(1,2,3)	0.017	118.64	4.46	4.41	4.50	0.86	0.85	0.87
t26w2h1.5-t(1,2,3)	0.017	118.86	4.35	4.40	4.45	0.90	0.91	0.92
t22w0.5h0.5-c(1,2,3)	0.029	18.13	3.65	3.85	3.67	1.13	1.20	1.14
t22w0.5h0.5-ct(1,2,3)	0.029	18.35	3.42	3.29	3.58	1.18	1.13	1.23
t22w0.5h0.5-t(1,2,3)	0.029	17.93	2.99	2.90	3.02	1.15	1.12	1.16
t22w1h0.75-c(1,2,3)	0.029	35.06	4.86	4.78	4.78	1.06	1.05	1.05
t22w1h0.75-ct(1,2,3)	0.029	35.40	4.44	4.34	4.55	0.99	0.97	1.02
t22w1h0.75-t(1,2,3)	0.029	35.04	3.73	3.94	3.92	1.06	1.12	1.11
t22w3h2-c(1,2,3)	0.029	103.33	8.04	8.25	8.34	0.86	0.88	0.89
t22w3h2-ct(1,2,3)	0.029	103.00	7.38	7.47	7.54	0.85	0.86	0.86
t22w3h2-t(1,2,3)	0.029	103.31	7.14	7.07	7.15	1.00	0.99	1.00
t22w5.5h3-c(1,2,3)	0.029	188.98	12.89	12.98	13.24	0.87	0.87	0.89
t22w5.5h3-ct(1,2,3)	0.029	189.74	12.31	12.43	12.13	0.82	0.83	0.81
t22w5.5h3-t(1,2,3)	0.029	189.95	12.12	12.07	11.94	0.91	0.91	0.90

Note: 1 inch = 25.4 mm. 1 kip = 4.448 kN. $M_{u,test}$ = Tested ultimate moment. $M_{y,100\%Fy}$ = Calculated yield moment by using 100% of the actual yield strength. All the calculated moments are determined based on the AISI Specification (AISI 1986).

Table 8 Tested Yield Moments and Ratios of Tested Yield Moment to Calculated Yield Moment

Specimens	Thickness (in.)	Average w/t	$M_{y,test}$ (kips-in) (test 1)	$M_{y,test}$ (kips-in) (test 2)	$M_{y,test}$ (kips-in) (test 3)	$M_{y,test}/M_{y,100\%Fy}$ (test 1)	$M_{y,test}/M_{y,100\%Fy}$ (test 2)	$M_{y,test}/M_{y,100\%Fy}$ (test 3)
t28w1.5h1-c(1,2,3)	0.015	103.13	--	--	2.35	--	--	0.85
t28w1.5h1-ct(1,2,3)	0.015	103.52	n/a	2.35	2.21	n/a	0.96	0.90
t28w1.5h1-t(1,2,3)	0.015	102.86	2.16	--	2.10	0.97	--	0.95
t26w0.5h0.5-c(1,2,3)	0.017	31.43	1.78	1.72	1.75	0.99	0.96	0.97
t26w0.5h0.5-ct(1,2,3)	0.017	31.33	1.72	1.92	1.77	1.02	1.14	1.05
t26w0.5h0.5-t(1,2,3)	0.017	31.65	1.63	1.80	1.65	1.11	1.23	1.13
t26w1h0.75-c(1,2,3)	0.017	61.07	2.16	--	--	0.96	--	--
t26w1h0.75-ct(1,2,3)	0.017	60.38	2.31	2.23	--	1.14	1.10	--
t26w1h0.75-t(1,2,3)	0.017	59.56	2.02	1.96	2.03	1.12	1.09	1.13
t26w2h1.5-c(1,2,3)	0.017	120.41	--	4.34	--	--	0.80	--
t26w2h1.5-ct(1,2,3)	0.017	118.64	4.26	--	4.42	0.82	--	0.85
t26w2h1.5-t(1,2,3)	0.017	118.86	--	--	4.41	--	--	0.91
t22w0.5h0.5-c(1,2,3)	0.029	18.13	3.44	n/a	3.29	1.07	n/a	1.02
t22w0.5h0.5-ct(1,2,3)	0.029	18.35	3.09	3.07	n/a	1.06	1.06	n/a
t22w0.5h0.5-t(1,2,3)	0.029	17.93	2.86	2.79	2.85	1.10	1.07	1.10
t22w1h0.75-c(1,2,3)	0.029	35.06	--	--	--	--	--	--
t22w1h0.75-ct(1,2,3)	0.029	35.40	4.44	4.29	4.54	0.99	0.96	1.02
t22w1h0.75-t(1,2,3)	0.029	35.04	3.66	n/a	3.72	1.04	n/a	1.05
t22w3h2-c(1,2,3)	0.029	103.33	--	8.16	--	--	0.87	--
t22w3h2-ct(1,2,3)	0.029	103.00	7.29	7.45	7.51	0.84	0.85	0.86
t22w3h2-t(1,2,3)	0.029	103.31	7.14	7.07	7.15	1.00	0.99	1.00
t22w5.5h3-c(1,2,3)	0.029	188.98	12.89	--	--	0.87	--	--
t22w5.5h3-ct(1,2,3)	0.029	189.74	--	--	12.13	--	--	0.81
t22w5.5h3-t(1,2,3)	0.029	189.95	--	--	--	--	--	--

Note: 1 inch = 25.4 mm. 1 kip = 4.448 kN. $M_{y,test}$ = Tested yield moment. $M_{y,100\%Fy}$ = Calculated yield moment by using 100% of the actual yield strength. "--" = Panel did not yield in the section according to the recorded strains. "n/a" = Data not available. All the calculated moments are determined based on the AISI Specification (AISI 1986).
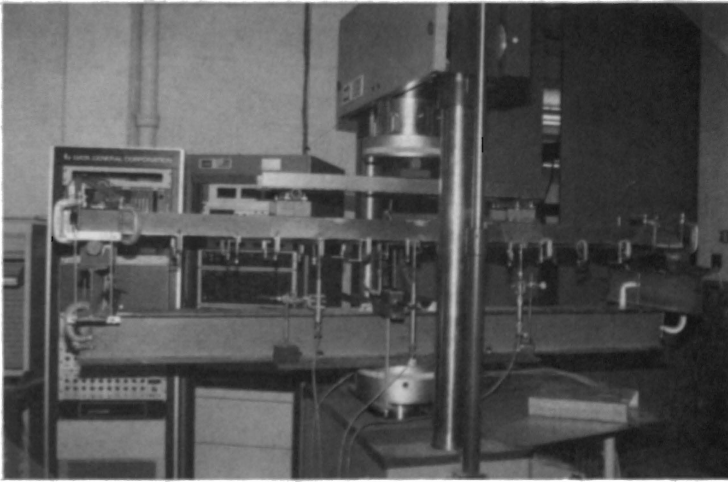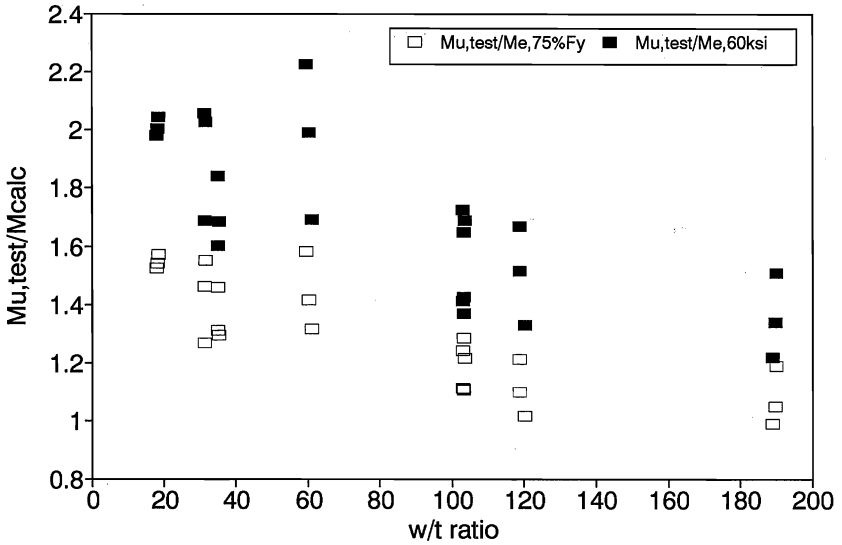
Figure 3 Test Setup

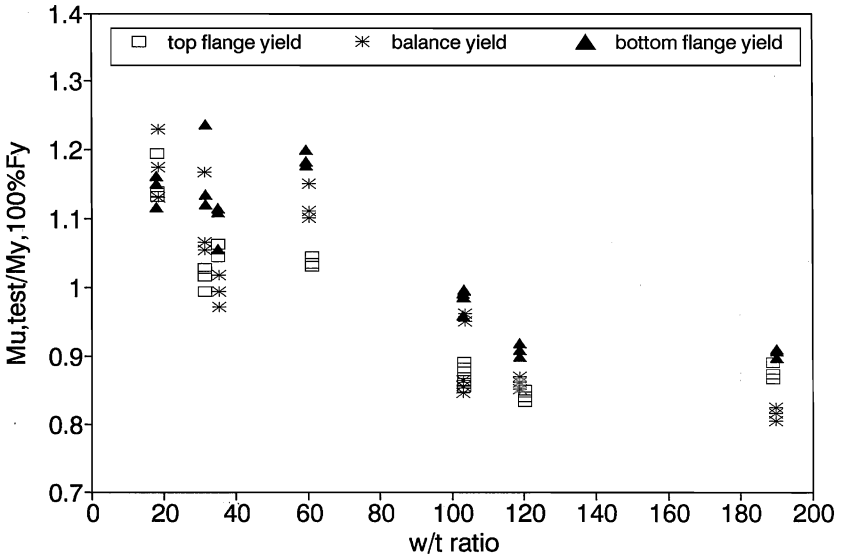Figure 4 Ratio of Tested Ultimate Moment to Calculated Moment vs. w/t Ratio

Figure 5 Ratio of Tested Ultimate Moment to Calculated Yield Moment vs. w/t Ratio
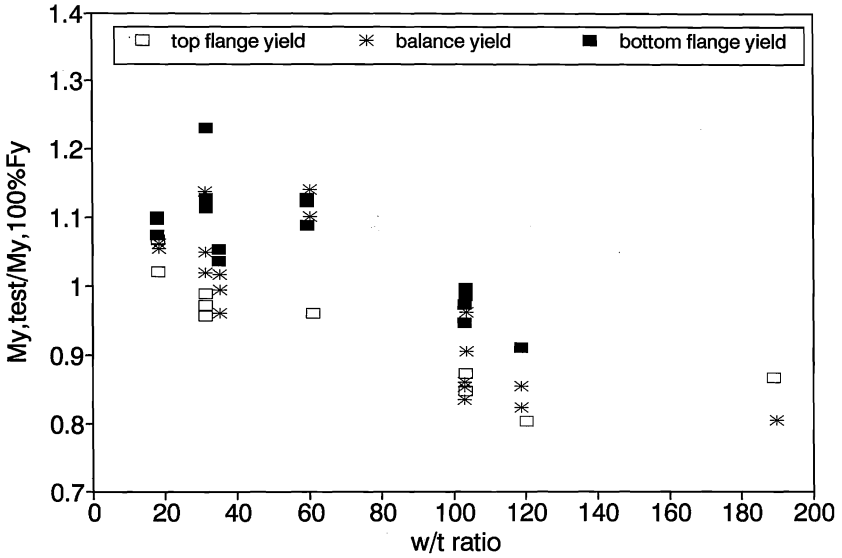
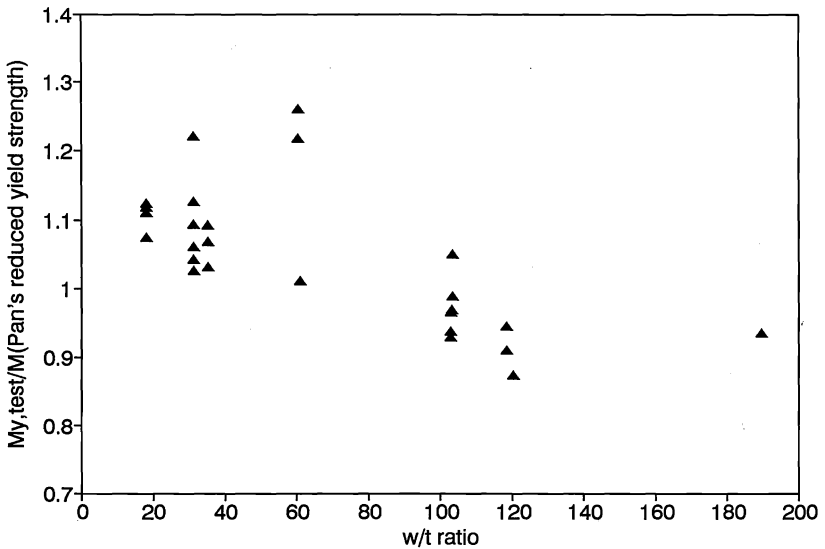Figure 6 Ratio of Tested Yield Moment to Calculated Yield Moment vs. w/t Ratio

Figure 7 Ratio of Tested Ultimate Moment to Calculated Moment Using Reduced Yield Strength vs. w/t Ratio